Clinical Study

Stereotactic and Functional Neurosurgery

Stereotact Funct Neurosurg 2012;90:161–166
DOI: 10.1159/000336754

Received: July 3, 2011
Accepted after revision: January 19, 2012
Published online: April 11, 2012

# Capability of Identifying Red Nuclei in Different Pulse Sequences of Regular 1.5-Tesla Magnetic Resonance Images

Shang-Ming Chiou[a, c] Yu-Chien Lo[b, c] Hung-Lin Lin[a]

Departments of [a]Neurosurgery and [b]Neuroradiology, China Medical University Hospital, and [c]School of Medicine, College of Medicine, China Medical University, Taichung, Taiwan

**Key Words**
Deep brain stimulation · Magnetic resonance image · Pulse sequence · Red nucleus · Subthalamic nucleus

**Abstract**
***Objective:*** To investigate the optimal pulse sequences of commonly used 1.5-tesla MRI for identifying the red nucleus (RN) to aid targeting of the subthalamic nucleus (STN). ***Methods:*** Forty-six healthy adults were enrolled for this prospective study. All subjects underwent MR studies of 5 sequences: diffusion-weighted imaging (DWI), $T_1$-weighted fluid-attenuated inversion recovery (T1IR), fast spin echo $T_2$-weighted imaging (FSE-T2WI), $T_2$-weighted fluid-attenuated inversion recovery (T2FLAIR) and $T_2$*-weighted gradient-echo (T2*-GRE) sequences. The clearness of the RN contour was analyzed. ***Results:*** Overall, the RN was identified in 98% subjects without gender and age differences. The RN was demarcated on a 5-mm slice relatively better in T2FLAIR (93.5%), followed by FSE-T2WI (78.3%), T2*-GRE (65.2%) and DWI (43.5%) sequences, but was completely invisible on the T1IR image. Generally, the signal intensity in all MR sequences decreased mildly on 2-mm slices with a similar identifying power. The detecting power on 5-mm slices was in favor of T2FLAIR with 94% sensitivity, 10% specificity, and 1.89 odds ratio compared to FSE-T2WI. In addition, the scanning time of T2FLAIR was longer in comparison to the FSE-T2WI study. ***Conclusion:*** T2FLAIR is an alternative to FSE-T2WI that can readily demarcate the RN to help target the STN.



## Introduction

Accurate stereotactic placement of the electrode within the subthalamic nucleus (STN) is imperative to the therapeutic success of deep brain stimulation surgery for Parkinson's disease (PD) [1]. However, the pre-/postoperative localization of the STN is a challenging issue because of its variable orientation and relatively small volume (approximately 240 $mm^3$) [2]. The STN is not visible in ventriculography or computed tomography scanning [3]. Traditionally, coordinates of the STN were indirectly determined, based on the Schaltenbrand and Wahren atlas [4], in relation to the visible landmarks such as the anterior commissure and the posterior commissure [1, 3, 5]. However, the borders, size, and shape of the STN in reference to the anterior commissure/posterior commissure points change significantly with age [6], irrespective of gender, side of the brain, and length of the anterior

KARGER

Fax +41 61 306 12 34
E-Mail karger@karger.ch
www.karger.com


1011–6125/12/0903–0161$38.00/0

Accessible online at:
www.karger.com/sfn

Dr. Shang-Ming Chiou
Department of Neurosurgery, China Medical University Hospital
2, Yuh-Der Road
Taichung, Taiwan (Republic of China)
Tel. +886 4 2205 2121, ext. 5040, E-Mail tsmchiou@pchome.com.tw

**Table 1**. Parameters of the 5 MR pulse sequences used in this study and the changes of signal intensity and median scanning time of 5 MR sequences by 2-mm thickness imaging

| Sequence | DWI | T1IR | FSE-T2WI | T2FLAIR | T2*-GRE |
|---|---|---|---|---|---|
| Parameters | | | | | |
| TR, ms | 6,300 | 2,400 | 4,000–5,500 | 9,000 | 600 |
| TE, ms | 84 | 24 | 100 | 130 | 22 |
| TI, ms | – | 750 | – | 2,250 | – |
| Matrix, mm | 128 × 128 | 320 × 256 | 384 × 256 | 320 × 224 | 288 × 224 |
| Thickness, mm | 5 | 5 | 5 | 5 | 5 |
| 2-mm thickness imaging | | | | | |
| SNR, % | 17 | 70 | 66 | 57 | 54 |
| Scanning time (median) | 1′41″ | 3′52″ | 1′18″ | 4′12″ | 2′55″ |

TR = Pulse repetition time; TE = echo delay time; TI = inversion time; SNR = signal intensity to noise ratio.

commissure-posterior commissure line, which remains almost constant [6].

The biconvex-shaped STN is obliquely located in the upper part of the mesencephalon, immediately cranial to the substantia nigra, cranio-postero-medial to the cerebral peduncle, and cranio-antero-lateral in 1.5- to 3-mm spatial width to the red nucleus (RN) [2, 7]. There is a short transitional zone where the mediodorsal border of the STN and the lateral border of the RN overlap each other. The anterior border of the RN approximately corresponds to the center of the STN along the cranio-caudal axis [7]. In magnetic resonance (MR) images, these 3 subcortical nuclei are delineated as dark (hypointense) area in various signal visibility [1, 7, 8].

At present, many centers adapt the 1.5-tesla axial $T_2$-weighted MR images to directly recognize the STN [1, 3, 5, 9]. However, this direct targeting method is not always possible or satisfactory, especially in the distorted coronal cut [3, 5, 9]. The boundary between the STN, substantia nigra and medial surrounding nuclei is very narrow and always blurry, making it difficult to discriminate clearly one from the other all the time [3, 5, 7]. It is necessary to find other imaging modalities or targeting methods to achieve satisfactory clinical outcome. Although some authors advocated that the STN could be reliably detected using 3-tesla MR images [8, 9], this technique is not popularly available in most centers. In addition, the compatibility of electrodes has not been extensively tested for 3-tesla MR scanners.

The RN is much larger and relatively easier to be identified than the STN. In 2005, Andrade-Souza et al. [5] demonstrated that the RN-based method using axial fast spin-echo $T_2$-weighted images (FSE-T2WI) could help to precisely target the STN with great reliability. The STN was defined with the x-coordinate 3 mm lateral to the most lateral border of the RN, and the y-coordinate the same as that of the anterior border of the RN in the axial plane. The z-coordinate is 2 mm inferior to the superior border of the RN in the coronal plane [5]. This technique is now well adapted in many centers. To the best of our knowledge, the actual identification rate of the RN by routinely used MR sequences has not been reported previously. We hypothesize that pulse sequences other than FSE-T2WI could also be applied on some occasion to better outline the RN. The present study will also attempt to address the role of gender or aging process on RN detecting ability.

## Materials and Methods

Forty-six healthy subjects, admitted for annual health examinations, were enrolled for this two-stage prospective study. There were 23 men and 23 women, with a mean age of 53 years (range 33–79). None of the participants suffered from any major medical, neurologic, or neuropsychiatric disorders. Subjects with small infarcts or foci of ischemia on MR images were excluded. The study complied with institutional guidelines and regulations and was approved by the local ethics committee.

During the initial study, all subjects underwent routine non-contrast MR studies of the whole brain using a 1.5-tesla Signa Excite HDx (General Electric Medical Systems) screener in 5 different sequences: diffusion-weighted imaging (DWI), $T_1$-weighted inversion recovery (T1IR) sequence, FSE-T2WI sequence, $T_2$-weighted fluid-attenuated inversion recovery (T2FLAIR) and $T_2$*-weighted gradient-echo (T2*-GRE) imaging. The MR images were obtained in an axial orientation of 5-mm thickness without gap (table 1).

During the second stage of the study, we randomly assigned 10 of these subjects to undergo scanning identical to ordinary stereo-

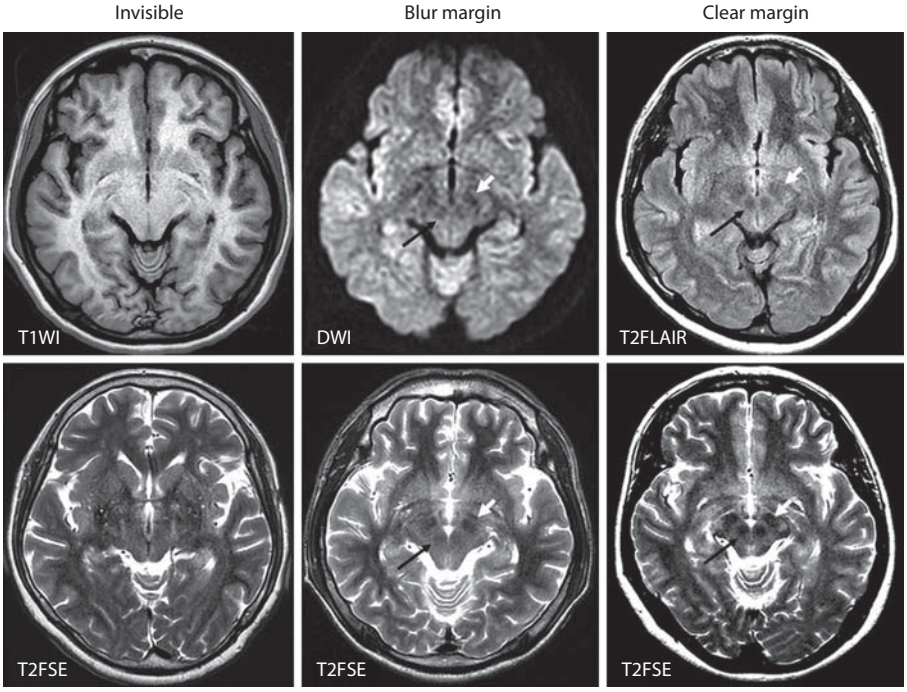


**Fig. 1.** Examples of categorizing margin contour of the RN (long thin arrow) in the different 1.5-tesla MR sequences used in this study. Note that the STN (short white arrow) is not always visible, and its size and boundary are highly variable or even unclear.

tactic procedures of 2-mm thickness in 256 × 256 matrices. The scanning parameters were not changed. The images cover only the segment from the level of the intercommissural line to the lower end of the pons, also in axial orientation without a gap. The caudal slices within the transitional zone of overlapped RN and STN were chosen to define the signal intensity of the RN.

The clearness of RN contour was categorized as follows: (1) RN was not visible; (2) RN was visible but its contour was blurred, and (3) RN was visible with a clear margin (fig. 1). A senior neurosurgical resident (Dr. Lin) and an independent senior neuroradiologist (Dr. Lo) verified simultaneously the correspondence of RN scoring without previous knowledge of the study purpose. The $\chi^2$ test served for comparison of categorized variables. A p value of less than 0.05 (two-tailed) was considered statistically significant. All the statistical analyses were performed with PASW Statistics 18 (SPSS Inc., Chicago, Ill., USA).

**Table 2.** Distribution of 46 persons by clearness of RN shown in 5 MR sequences of 5-mm thickness

| Sequence/contour | DWI | T1IR | FSE-T2WI | T2FLAIR | T2*-GRE |
|---|---|---|---|---|---|
| Invisible | 26 (56.5) | 46 | 10 (21.7) | 3 (6.5) | 16 (34.8) |
| Blur margin | 18 (39.1) | 0 | 29 (63.0) | 20 (43.5) | 28 (60.9) |
| Clear margin | 2 (4.3) | 0 | 7 (15.2) | 23 (50.0) | 2 (4.3) |
| Total | 46 | 46 | 46 | 46 | 46 |

Figures in parentheses indicate percentages.

## Results

Overall, the RN could be identified in 98% subjects, except in one 65-year-old woman revealing a completely invisible RN in all 5 MR studies. The case distribution of the entire series is shown in table 2, according to the clearness of the RN by different MR sequences. In general, the RN was completely invisible in T1IR images; in contrast, the $T_2$-weighted sequences had a better capability to outline the borders and position of the RN. The RN was displayed particularly brilliantly in T2FLAIR sequences if at all visible occasions ($p < 0.001$). The highest rate of RN demarcation was found in T2FLAIR (n = 43, 93.5%; $\chi^2 = 34.783$, $p < 0.001$), followed by FSE-T2WI (n = 36, 78.3%; $\chi^2 = 14.696$, $p < 0.001$), T2*-GRE (n = 30, 65.2%; $\chi^2 = 4.261$, p = 0.0391) and DWI (n = 20, 43.5%; $\chi^2 = 0.783$, p = 0.376) sequences. Notably, there were also some cases where the RN was not recognized on the FSE-T2WI (22%) or T2FLAIR (7%) sequence, and the RN margin can be distinguished more clearly in T2FLAIR than in FSE-T2WI (table 2).

Statistically, gender differences did not play any role on RN detecting ability, and aging process (a cutoff point of 50 years of age) did not increase the RN detection rate (table 3). If the FSE-T2WI was considered as a golden standard, then the detecting ability of T2FLAIR for the

**Table 3.** Differences of visible capability to outlining RN on routinely used MR sequences of 5-mm thickness by gender and by aging process

| | DWI | FSE-T2WI | T2FLAIR | T2*-GRE |
|---|---|---|---|---|
| Gender | | | | |
| Man | 9 (39.1%) | 18 (78.3%) | 23 (100%) | 15 (65.2%) |
| Woman | 11 (47.8%) | 18 (78.3%) | 20 (87.0%) | 15 (65.2%) |
| Statistics | $\chi^2 = 0.354$ p = 0.552 | – | $\chi^2 = 3.209$ p = 0.233 | – |
| Age | | | | |
| <50 years | 9 (45.0%) | 17 (85.0%) | 20 (100%) | 14 (70.0%) |
| ≥50 years | 11 (42.3%) | 19 (73.1%) | 23 (88.5%) | 16 (61.5%) |
| Statistics | $\chi^2 = 0.033$ p = 0.855 | $\chi^2 = 0.945$ p = 0.476 | $\chi^2 = 2.469$ p = 0.246 | $\chi^2 = 0.357$ p = 0.550 |

**Table 4.** Comparison of detecting ability of T2FLAIR to outlining RN with FSE-T2WI as a golden standard

| | FSE-T2WI | | | |
|---|---|---|---|---|
| | visible | none | total | |
| T2FLAIR | | | | |
| Visible | 34 | 9 | 43 | Sensitivity = 34/(34 + 2) = 94.4% |
| None | 2 | 1 | 3 | Specificity = 1/(1 + 9) = 10.0% |
| Total | 36 | 10 | 46 | Diagnostic accuracy = (34 + 1)/46 = 76.1% |
| | | | | Odds ratio = (34 × 1)/(9 × 2) = 1.89 |

RN was as follows: sensitivity 94%, specificity 10%, diagnostic accuracy 76% and odds ratio 1.89 (table 4). When we implemented a similar scanning of 2-mm thickness, the aforementioned findings were also applicable to the outline of the RN (fig. 2). However, the signal intensity decreased in all MR sequences (table 1); therefore, the RN was recognized relatively in worse quality. Nevertheless, the T2FLAIR and FSE-T2WI images still retained some acceptable signal intensity. Clearly, both the T2FLAIR and FSE-T2WI images are optimal for stereotactic application, although the acquisition time required for T2FLAIR images is longer than that of FSE-T2WI images (table 1).

## Discussion

Stereotactic functional surgical procedures represent interventions into a complex and delicate 3-dimensional brain space. The planning of a neurosurgical approach is directly related to the degree of surgical invasiveness and the overall therapeutic efficacy. The integration of all of the radioimaging information into a 3-dimensional context can be a difficult mental process especially if the surgical target is tiny and structurally difficult to access. The process becomes even more complex when numerous complementary imaging series are available but are different in slice thickness, scale, and patient orientation. For patients with movement disorders undergoing stereotactic procedures, the optimal MR sequences should be straightforward to distinguish details of the related nuclei. Also, a sequence of ideal MR requires a relatively short scanning time to avoid any patient discomfort and motion artifacts in an 'off-medication' state.

The present study showed that neither the STN nor the RN was always visible with a clear margin on routine or stereotaxis-oriented 1.5-tesla MR images, or even completely invisible in some cases regardless of the sequences used. Our analysis demonstrated that the RN is more easily recognized in the $T_2$-weighted sequences to a variable degree but was invisible in the T1IR sequence (table 2; fig. 1, 2). There were no significant differences in the RN detection rate between men and women or as a result of the aging process (older than 50 years old) for the entire

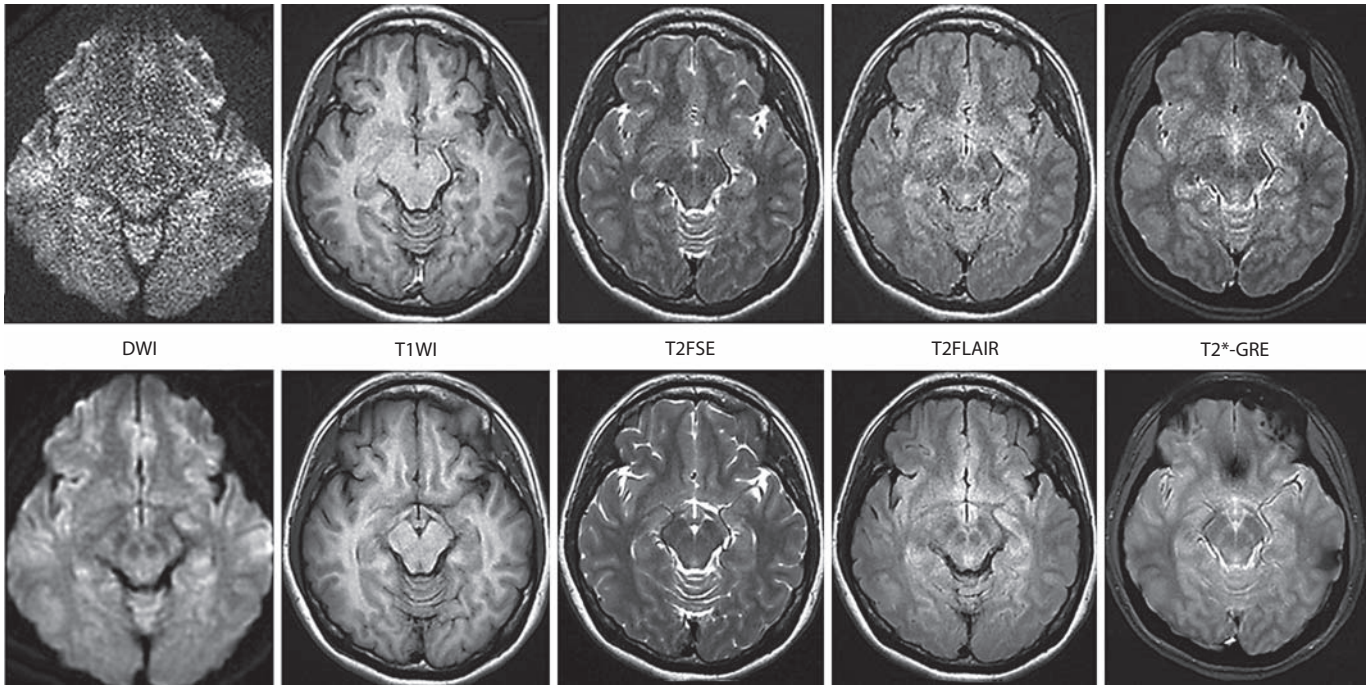


**Fig. 2.** Example of the different capability of different pulse sequences for identifying RN in 2-mm (**a**) and 5-mm (**b**) slice axial MR images in a 43-year-old healthy subject. Note that the signal-to-noise ratio fades to different degrees on all MR images of thinner thickness.

series (table 3). However, if the RN could be demarcated well, then the T2FLAIR and FSE-T2WI images were the two optimal choices of MR sequences especially in persons younger than 50 years of age. The detecting ability of T2FLAIR for the RN was relatively good with 94% sensitivity compared to FSE-T2WI as a golden standard (odds ratio, 1.89) (table 4). If MR images were acquired in thinner (2-mm) slices as in stereotactic procedures, the MR signal intensity would decrease due to a lower signal-to-noise ratio (poorer image contrast) (table 1; fig. 2). However, the RN was still well demarcated by both the FSE-T2WI and T2FLAIR images, although the scanning time was faster in the FSE-T2WI sequence. Obviously, the T2FLAIR sequence could serve as an alternative to define the RN for targeting STN, provided the commonly used FSE-T2WI images are not clear or invisible.

The slice thickness of MR images is commonly set to 2–5 mm for ordinary stereotactic procedures such as tumor biopsy; but conventionally confined to 2 mm for functional neurosurgery. Therefore, we designed a two-stage setting in our series. However, some limitations in the current study should be acknowledged. First, our scanning parameter protocols were set for screening in routine health examinations; not tailored for functional procedures or specially designed for detecting RN. There might be some other optimal sequences that can yield a better definition of the RN fairly well in clinical practice. For example, the TE value (22 ms) of T2*-GRE might be too short to delineate the RN boundary. Second, the optimizing parameters for setting FSE-T2WI and T2FLAIR images on thinner slices need to be further investigated for patients with advanced PD.

The hypointense signal of subcortical nuclei is attributed to regional- and age-dependent depositions of non-heme iron resulting in contrast differences between the white and gray matter [10, 11]. Biochemical studies have proposed that excessive iron deposition is an important biomarker in the pathophysiology of neurodegenerative disease [10, 12]. Recently, Zhang et al. [12] reported an in vivo case-control study using magnetic susceptibility-weighted phase MR imaging to clarify the correlation of brain iron accumulation with the clinical status in patients with PD. They found that there existed no significant difference in iron contents in the subcortical nuclei studied between the healthy controls and the PD patients, except in the substantia nigra ($p = 0.000$) [12]. Accord-

ingly, we suppose that the findings in the present study could also be applied to the PD patients.

The present study has proved that the direct RN-based targeting method is convincingly feasible to help target the STN for clinical applications. If the target has been anatomically located as precisely as possible, the need for multiple passes of the microelectrode for time-consuming detailed electrophysiologic confirmation can be theoretically reduced. Thereby, patient morbidities, such as hemorrhage, can be avoided or decreased. Moreover, the operation time will be shortened, especially if it is done bilaterally in a single setting. However, because MR images may be distorted to some degrees depending on the pulse sequence [3, 5], plus the STN and the RN are not always visible in some populations as noted in this study, we do affirm that image-based targeting alone is not sufficient to replace the role of intraoperative neurophysiological confirmation. We recommend using the RN-based method only as a starting point. Refinement of final optimal STN location for placing the deep brain stimulation electrodes should be decided by analyzing other integrated information including intraoperative electrophysiological recording, micro- or macrostimulation, and observation of its clinical and side effects [3].

## Conclusion

This prospective study investigated the clearness of the RN contour on routine or stereotaxis-oriented 1.5-tesla MR images. Our results demonstrated that the direct RN-based method on MR images is feasible to help target STN during deep brain stimulation surgery. Our results demonstrated that both T2FLAIR and FSE-T2WI images exhibited the strongest and optimal signal intensity of the RN. The detecting ability of RN was in favor of the T2FLAIR sequence with 94% sensitivity, 10% specificity; however, the scanning time was faster in the FSE-T2WI sequence if the MR image was acquired in thinner slices. We suggest that the T2FLAIR sequence can be used as an alternative to define the RN for targeting STN, provided the commonly used FSE-T2WI images of STN is not clear. Further study is warranted especially in functional surgery for PD patients.


## Acknowledgement

This study was supported in part by Taiwan Department of Health Clinical Trial and Research Center of Excellence (DOH100-TD-B-111-004).


## References


1 Zonenshayn M, Sterio D, Kelly PJ, Rezai AR, Beric A: Location of the active contact within the subthalamic nucleus (STN) in the treatment of idiopathic Parkinson's disease. Surg Neurol 2004;62:216–225.

2 Hamani C, Saint-Cyr JA, Fraser J, Kaplitt M, Lozano AM: The subthalamic nucleus in the context of movement disorders. Brain 2004; 127:4–20.

3 Breit S, LeBas J-F, Koudsie A, Schulz J, Benazzouz A, Pollak P, Benabid A-L: Pretargeting for the implantation of stimulation electrodes into the subthalamic nucleus: a comparative study of magnetic resonance imaging and ventriculography. Neurosurgery 2006;58:ONS83–ONS95.

4 Schaltenbrand G, Wahren W: Atlas for Stereotaxy of the Human Brain. Stuttgart, Thieme, 1977.

5 Andrade-Souza YM, Schwalb JM, Hamani C, Eltahawy H, Hoque T, Saint-Cyr J, Lozano AM: Comparison of three methods of targeting the subthalamic nucleus for chronic stimulation in Parkinson's disease. Neurosurgery 2005;56:360–368.

6 den Dunnen WFA, Staal MJ: Anatomical alterations of the subthalamic nucleus in relation to age: a postmortem study. Mov Disord 2005;20:893–898.

7 Rijkers K, Temel Y, Visser-Vandewalle V, Vanormelingen L, Vandersteen M, Adriaensen P, Gelan J, Beuls EA: The microanatomical environment of the subthalamic nucleus. Technical note. J Neurosurg 2007;107:198–201.

8 Slavin KV, Thulborn KR, Wess C, Nersesyan H: Direct visualization of the human subthalamic nucleus with 3T MR imaging. Am J Neuroradiol 2006;27:80–84.

9 Toda H, Sawamoto N, Hanakawa T, Saiki H, Matsumoto S, Okumura R, Ishikawa M, Fukuyama H, Hashimoto N: A novel composite targeting method using high-field magnetic resonance imaging for subthalamic nucleus deep brain stimulation. J Neurosurg 2009; 111:737–745.

10 Martin WR: Quantitative estimation of regional brain iron with magnetic resonance imaging. Parkinsonism Relat Disord 2009; 15(suppl 3):S215–S218.

11 Aquino D, Bizzi A, Grisoli M, Garavaglia B, Bruzzone MG, Nardocci N, Savoiardo M, Chiapparini L: Age-related iron deposition in the basal ganglia: quantitative analysis in healthy subjects. Radiology 2009;252:165–172.

12 Zhang J, Zhang Y, Wang J, Cai P, Luo C, Qian Z, Dai Y, Feng H: Characterizing iron deposition in Parkinson's disease using susceptibility-weighted imaging: an in vivo MR study. Brain Res 2010;1330:124–130.